

The Effect of Steel Reinforcement Number on the Resistance of Rail Sleepers of Passenger Railway

Dhani Ryandhi¹, Andhi Idhil Ismail^{1,2*}, Faisal Manta¹

¹Department of Mechanical Engineering, Institut Teknologi Kalimantan, Balikpapan, Indonesia

²National Center for Sustainable Transportation Technology, Bandung, Indonesia

*Email: a.idhil@lecturer.itk.ac.id

Abstract

The train is a mode of transportation that offers characteristics and advantages because of its ability to transport passengers and goods in bulk, efficiently, sparingly on space use, and safely. The comfort and safety of the train cannot be separated from the structure of the train and the existing rail structure. A railway system generally consists of train buildings (carriages) and railroads. The rail structure consists of the rail itself, under which there are railway sleepers and a foundation or ballast. The sleeper serves as the foundation on which the rail rests. The materials used for sleepers are of various kinds, such as wood, steel, or reinforced concrete. Concrete or reinforced concrete with tension steel helps receive a load from the train tracks and wheels. Therefore, the sleepers can withstand impact loads. This study aims to analyze the effect of impact loads and sleeper reinforcement variations on railway sleepers' resistance. Finite Element Analysis (FEA) is used to model and analyze the sleeper performance after impact loading. The variety of reinforcement used is 4, 6, and 8 rods with 7-type formations. The results that can be obtained are in the form of stress, load, and displacement values. The value of the stress on the whole system is 1860 MPa. The maximum load value is 245.33 kN for variations of 6 reinforcements formations 1. The displacement value is 14.03 mm. The simulation results and graphs show that the correct arrangement and number of reinforcements can increase the resistance of the railway sleeper.

Keywords

Finite element analysis; Railway sleeper; Sleeper reinforcement.

1 Introduction

The train is one of the modes of transportation with characteristics and advantages because of its ability to transport passengers and goods in bulk, efficiently, sparingly on space use, and safely. The train is a type of mass transportation consisting of a locomotive and a series of trains or carriages. The series of trains or carriages are relatively large, so they can load passengers and goods on a large scale. Because it is very effective mass transportation, the Indonesian government is trying to use it as the primary means of land transportation within and between cities through the Ministry of Transportation. Railways offer distinctive qualities and benefits, particularly in their capacity to convey large quantities of people and commodities, conserve energy, reduce the need for space, increase safety, reduce pollution, and outperform other forms of land transportation.

Railway track sleepers assume a considerable part in the strength and stability of the rail track. The sleepers' principal function is to support rail powers and move them as consistently as conceivable to the ballast bed. Railway operators are interested in further increasing

sleeper life because of the increase in the axle loads, speed, and traffic volumes in the railway transport systems, causing significant expenses for sleeper maintenance and substitution [1], [2]. In the new age of high-speed tracks, two factors of sleeper implementation need further examination: cracks in sleepers and sleepers' role in instigating track vibrations. Cracks in sleepers have been investigated in the literature. These cracks are chiefly owing to substantial sleeper material weakness, especially when the unique burden causes the track construction to resonate. As a result, the cracks reduce sleeper life [3]–[5]. Sleeper cracks and track-induced vibration are the main issues in high-speed tracks. However, adequate hypothetical and trial studies on sleepers' energy retention and lifespan are limited. This paper tries to address this issue. It has been demonstrated that adding steel tendons to concrete structures can increase their stiffness, flexural strength, fatigue strength, energy absorption limit, and protection from cracking. Works investigating the crack have been done in limited variation. However, the cost of experimental works [6], [7] is high and requires a longer time to prepare a variation of railway sleepers. Therefore, it is necessary to investigate railway sleepers with the variation of steel

tendons using state-of-the-art finite element analysis (FEA). FEA is an excellent technique for simulating and analyzing complex structural scenarios since it provides knowledge that might be used to fix issues without using as many resources as conventional experimental methods.

The comfort and safety of the train cannot be separated from the structure of the train and the existing rail structure. A railway system generally consists of trains (carriages) and railroad tracks. The railroad structure consists of 2 parts, the upper structure, namely the track section consisting of rails, sleepers, and rail fastenings, and the lower structure, namely the foundation section consisting of ballast and subgrade. The rail functions as a track for the train wheels to be the first part of receiving pressure from the wheels. Furthermore, rail fasteners function so that the sleepers remain attached to the rail sleepers. The sleeper serves as the foundation on which the rail rests. The materials used for sleepers are of various kinds, such as wood, steel, or reinforced concrete. Due to the sleepers that receive the load from the train wheels, prestressed rebar concrete is used or concrete with tension steel which is helpful so that the load from the train wheels can be neutralized so that the sleepers can withstand impact loads. This work examines the structure of the upper part, especially on the railroad sleepers. This research will utilize Finite Element Analysis (FEA) to model railroad sleepers by varying the reinforcement for 4, 6, and 8 bars with several different formations to determine the effect of variations in the amount of reinforcement on sleeper resistance after obtaining a load.

2 Methodology

2.1 Finite element method (FEM) modeling

This work used a brittle cracking model [8], [9], already implemented in ABAQUS. The model allows for simulating crack propagation in the sleeper when impact loading is applied. The sleeper model in this study refers to the sleepers manufactured by CEMEX, a Mexican multinational building materials company that produces and distributes cement, ready-mix concrete, and aggregates. The reinforcement used is a prestressed steel tendon with a diameter of 5 mm. The sleeper dimensions can be seen in Table 1.

The sleeper has a total length of 2520 mm. In the model, only half of the sleepers were used. Therefore, the length of the sleeper model was 1260 mm. The w_r is the width of the sleeper on the rail seat, d_r is the sleeper's height on the rail seat, w_c is the width at the sleeper's center, and d_c is the sleeper's height in the center of the sleeper. In this work, the sleeper model used can be seen in Figure 1, whereas the variations used for investigation are shown in Figure 2.

Table 1 Sleeper Dimension

Height (mm)	Total Length (mm)	Rail Seat (mm)		Center of Sleeper (mm)	
		w_r	d_r	w_c	d_c
200	2520	200	200	212	171

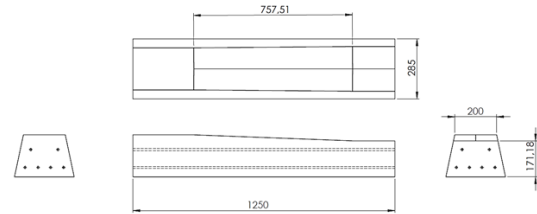


Figure 1 Design of concrete sleeper.

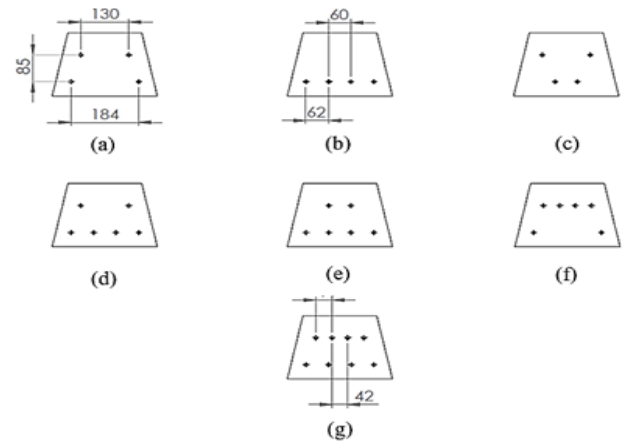


Figure 2 Variable amount and formation of prestressed steel reinforcement for (a) 4 reinforcements formation 1, (b) 4 reinforcements formation 2, (c) 4 reinforcements formation 3, (d) 6 reinforcements formation 1, (e) 6 reinforcements formation 2, (f) 6 reinforcements formation 1, and (g) 8 reinforcements.

The sleeper, rail, and wheels were modeled as shown in Figure 3. The model uses a C3D8R element type with 8 node points, while the sleeper reinforcement section uses a C3D6 element type with 6 node points. The selection of the type of element used is referenced from the literature [10]. The meshing results are demonstrated in Figure 3, whereas the number and size of elements of each part can be seen in Table 2. The loading is defined as an impact load with 600 kg as the mass of the train wheels and from a height of 200 mm because it conforms to the experimental studies previously carried out by [11]. The velocity for the collision used was 1940 mm/s, calculated from 98% of the capacity impact testing machine based on high-speed camera tests [11]. The loading conditions are adjusted to the simulation parameters carried out by [8].

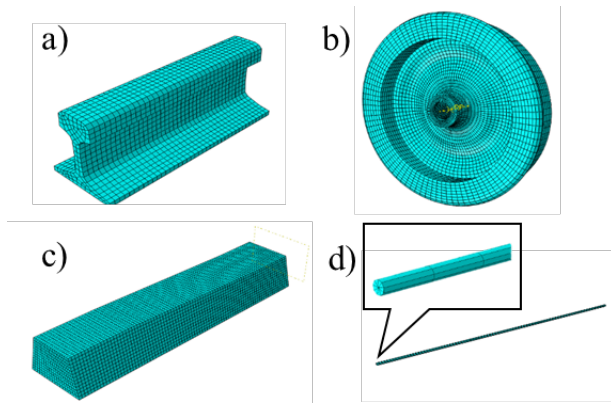


Figure 3 Meshed part of (a) rail, (b) wheel, (c) sleeper, and (d) sleeper reinforcement.

Table 2 Element Size and Total Element for Each Part

Part	Element Size (mm)	Total Element
Sleeper	15	19422
Rail	10	3600
Wheel	12	16074
Reinforcement	35	324

2.2 Material properties

The material used for the sleeper is high-strength concrete C50/60. The material properties of concrete, steel for wheels, rails, and sleeper reinforcement be seen in Table 3.

Table 3 Properties for Concrete and Steel

Properties	Concrete C50/60	Steel
Density	2.4 g/cm ³	7.8 g/cm ³
Young's Modulus	36406 MPa	200000 MPa
Poisson's Ratio	0.2	0.3
Compressive Strength	50 MPa	-
Tensile Strength	2.85 MPa	-
Fracture Energy	154 m	-

3 Results and discussion

3.1 Model validation

The model is validated to ensure the validity of the model and the results. The model used in the simulation is validated by comparing the results with previous experiments and simulations with the same parameters. Validation was carried out by referring to the research results from the literature [8], [11] by comparing the simulation results with the parameters associated with the study. The load-displacement graph comparing the simulation results is obtained, as shown in Figure 4 below.

Figure 4. compares the results of research simulations in journals represented in blue, where the maximum load value is 326.4 kN with a displacement value of 26.858 mm. The validation results obtained a maximum load value of 326.2 kN with a displacement value of 24.44 mm.

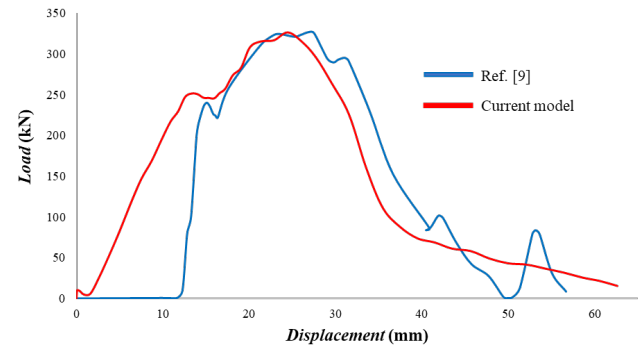


Figure 4 Load-displacement 6 reinforcements no hole sleeper comparison graph.

From the graph (Figure 4), it can be concluded that there is a positive correlation between the validation results of research [8]. The two results show a difference in the load value of 0.2 kN, estimated to occur due to the difference in the measurement location between the simulation and journal.

3.2 Crack propagation

The impact load on the rail sleeper above causes the crack to occur. Figure 5 demonstrates the failed sleeper at a step time of 0.025. It is due to tensile stress on the sleeper when receiving impact loads, while the tensile stress that occurs is 620.1 MPa, exceeding the sleeper tensile strength limit of 2.85 MPa [12-13].

The initial crack that occurs at the support (Figure 6) is a crack that propagates diagonally during the simulation process. It happens in every case, resulting in sleeper failure, as shown in Figure 7. This phenomenon indicates that sleepers lack resistance to tensile stress. Cracks on the sleepers indicate that the applied load generates stress that exceeds the tensile stress limit of the sleepers, causing failure. The crack propagation also shows similar patterns to the experimental results [3]. Although the initial crack propagation profile shows a similar form, the final failure shape of the sleeper demonstrates a distinctive look depending on the tendon formation. It highlights the influence of tendon reinforcement formation in absorbing and distributing the stress after impact loading.

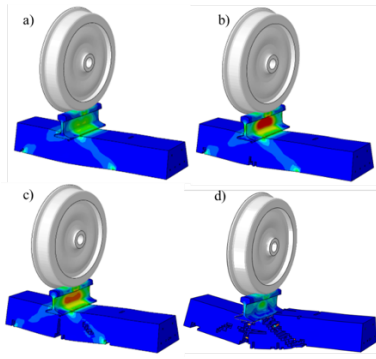


Figure 5 Crack propagation at step time(s) of (a) 0.010, (b) 0.0125, (c) 0.015, and (d) 0.025.

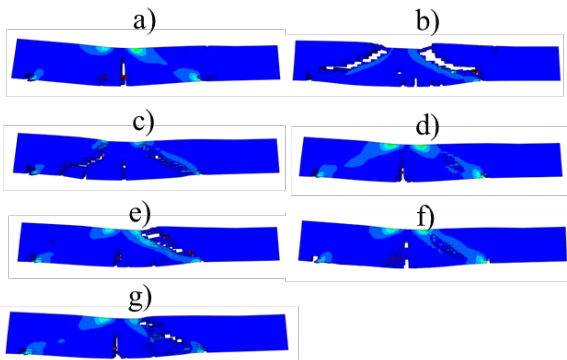


Figure 6 Simulation result at 0.015 s step time for (a) 4 reinforcements formation 1, (b) 4 reinforcements formation 2, (c) 4 reinforcements formation 3, (d) 6 reinforcements formation 1, (e) 6 reinforcements formation 2, (f) 6 reinforcements formation 3, and (g) 8 reinforcements.

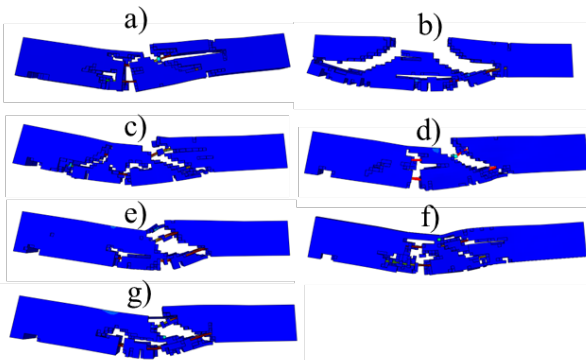


Figure 7 Simulation result at 0.025 s step time for (a) 4 reinforcements formation 1, (b) 4 reinforcements formation 2, (c) 4 reinforcements formation 3, (d) 6 reinforcements formation 1, (e) 6 reinforcements formation 2, (f) 6 reinforcements formation 3, and (g) 8 reinforcements.

In Figure 7, each sleeper case has an identical crack pattern at a step time of 0.015 s, except in Figure 7(b). The sleeper contains 4 reinforcements for formation 2 (Figure 7), which shows larger cracks than the other variations. The larger crack size is due to the lack of supporting reinforcement around the rail holder. Thus, the stress is easier to propagate on the sleepers. Some

other variations have supporting reinforcement around the rail holder and the sleeper holder.

Simulation results at 0.025 s step time can be seen in Figure 7, demonstrating different crack patterns in all sleepers' cases due to the variation in the number of steel reinforcements and their position on the sleepers. The crack variation occurs because the stresses originating from the steel reinforcement are spread at different sleeper points, causing different crack patterns. The maximum stress value occurs in each 1860 MPa contained in the prestressed steel reinforcement.

Figure 8 shows the load evolution during the simulation, in which the load increases at a step time of 0.004 s. From 0.004 s to 0.010 s, all sleepers' models experienced deflection but were still within the elastic limit of the sleepers, so cracking had not occurred. Since sleepers can be used before they are damaged or cracked to determine their resistance, the maximum load is seen before the sleeper's cracks so that sleepers' performance can be determined. The worst performance is seen in 4 reinforcement formation 2 with a maximum acceptable load of 205.53 kN at a step time of 0.009 s. The best performance is found in 6 reinforcement formations 1 with a maximum acceptable load of 245.33 kN. It can be seen in Figure 7 that the sleepers with a variation of 6 reinforcement formations at a step time of 0.015 s have a relatively smoother crack than the other variations.

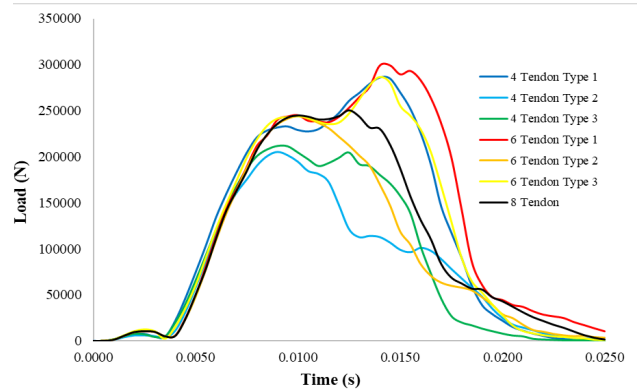


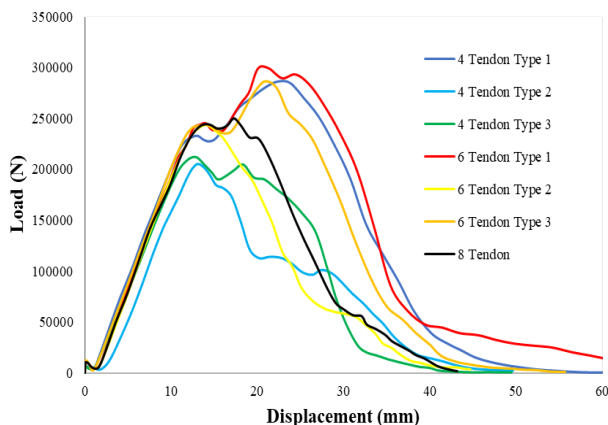
Figure 8 Load-time graph for each sleeper's variation.

The sleeper with 4 formation reinforcements 1 and 6 formation reinforcements 1 and 3 is still experiencing an increase in load because, in Figure 8 and Figure 9, three variations have not broken in the rail seat area after experiencing an increase in load up to a step time of 0.0145 s.

The load reduction was faster in 4 formations 2 and 3 reinforcements, 6 formations 2 reinforcements at a step time of 0.010 s, and 8 reinforcements at a step time of 0.013 s. When the sleepers receive the impact load, the first displacement up to the displacement at

12 mm still shows a linear pattern. However, the load at the failure onset shows different displacements. In the 4 reinforcements formation 1, the rail sleepers have failed with a maximum load of 220 kN and a displacement of 13.07 mm. A similar failure mode occurs in the variation of 6 reinforcements formations 1 and 3. However, the 8 reinforcements still experienced an increase in load up to 245 kN, with displacement of 14.03 mm, 14 mm, and 14.02 mm, respectively. The variation of 4 reinforcements formations 2 and 3, 6 reinforcements formation 2 has experienced a decrease in loading after reaching 211 kN because the sleepers had cracked to the rail seat with a displacement of 12.46 mm, 12.39 mm, and 13.97 mm, respectively (Figure 9).

The highest load value is found in the sleepers with 6 reinforcement formations 1 with a value of 245.33 kN. Not only by reducing or adding the number of reinforcements to determine the increase in the load that the sleepers can accept but it can also be seen in the 6 reinforcements formation 1, the load obtained is 245.33 kN, which is greater than the variation of 8 reinforcements which has a load of 244.86 kN. In this experiment, another aspect that can affect the magnitude of the load is the formation of reinforcements [14]; each variation of reinforcements with different formations has a different maximum load value. As in sleepers with 4 reinforcements, even though they have the same amount, the load received differs for each arrangement of reinforcements. The same phenomenon also appears in the sleepers with 6 reinforcements. Compared to the reference [9], the results obtained in the sleeper with 6 reinforcements show higher stress capacity. It can be achieved by substituting the hole with tendon reinforcement. It can be concluded that the amounts of reinforcements and their formation can affect the resistance of the railroad



sleepers, so it becomes an essential point in the design of the rail sleepers.

Figure 9 Load-displacement graph for each sleeper's variation.

4 Conclusion

The study of the effect of the amounts of reinforcements on the passenger rail sleepers on the resistance of the railroad sleepers using the finite element method has been successfully carried out. The analysis results show that the maximum stress for each case of the rail sleepers of 1860 MPa contained in the reinforcements as a support for the rail sleepers. Stress and crack distribution patterns are different in each case due to differences in the number of sleepers and reinforcements formations. The initial stress from the sleeper reinforcements spread across the rail sleepers affects the performance of the rail sleepers resulting in different loads received in each variation. The best performance can be seen in the sleepers with 6 reinforcements formation 1 with an acceptable load of 245.33 kN with a displacement value of 14.03 mm. It is necessary to follow up the simulation with experimental trials with selected configurations, especially sleepers with 4 and 6 reinforcements.

Acknowledgments

The authors acknowledge National Center for Sustainable Transportation Technology (NCSTT).

References

- [1] H. Yu, D. Jeong, J. Choros, and T. Sussmann, "Finite Element Modeling of Prestressed Concrete Crossties With Ballast and Subgrade Support," *International Design Engineering Technical Conferences and Computers and Information in Engineering Conference*, vol. 54815, pp. 1077–1086, 2011.
- [2] S. Li, "Railway Sleeper Modelling with Deterministic and Non-deterministic Support Conditions," *KTH Eng.*, 2012.
- [3] A. Remennikov and S. Kaewunruen, "Resistance of Railway Concrete Sleepers to Impact Loading," *Engineering*, 2007.
- [4] S. Kaewunruen and A. M. Remennikov, "Dynamic Crack Propagations in Prestressed Concrete Sleepers in Railway Track Systems Subjected to Severe Impact Loads," *J. Struct. Eng.*, vol. 136, no. 6, pp. 749–754, 2010.
- [5] S. Kaewunruen, A. Remennikov, and A. Aikawa, "A numerical study to evaluate dynamic responses of voided concrete Railway Sleepers to Impact Loading," 2011.
- [6] S. Kaewunruen and A. M. Remennikov, "Progressive failure of prestressed concrete sleepers under multiple-intensity impact loads," *Eng. Struct.*, vol. 31, no. 10, pp. 2460–2473, 2009.
- [7] D. L. Logan, *A First Course in the Finite Element Method*. Thomson, 2007.
- [8] O. C. Zienkiewicz and R. L. Taylor, *The Finite Element Method Set*, Elsevier, 2005.
- [9] S. Kaewunruen, C. Ngamkhanong, and C. H. Lim, "Damage and failure modes of railway prestressed concrete sleepers with holes/web openings subject to impact loading conditions," *Eng. Struct.*, vol. 176, pp. 840–848, 2018.
- [10] A. Parvez and S. J. Foster, "Fatigue of steel-fibre-reinforced concrete prestressed railway sleepers," *Eng. Struct.*, vol. 141, pp. 241–250, 2017.

- [11] S. Kaewunruen and A. M. Remennikov, "Structural Safety of Railway Prestressed Concrete Sleepers," vol. 9, no. 2, pp. 129–140, 2009.
- [12] M. Shin, Y. Bae, and S. Pyo, "A Numerical Study on Structural Performance of Railway Sleepers Using Ultra High-Performance Concrete (UHPC)," *Materials*, vol. 14, no. 11, p. 2979, 2021.
- [13] A. Ahmed, "Modeling of a reinforced concrete beam subjected to impact vibration using ABAQUS," *Int. J. Civ. Eng.*, vol. 4, no. 3, pp. 227–236, 2014.
- [14] J. Sadeghi, A. R. T. Kian, and A. S. Khabbazi, "Improvement of Mechanical Properties of Railway Track Concrete Sleepers Using Steel Fibers," *J. Mater. Civ. Eng.*, vol. 28, no. 11, p. 04016131, 2016.